Density functional theory and enzyme studies support interactions between angiotensin receptor blockers and angiotensin converting enzyme-2: Relevance to coronavirus 2019

Apostolopoulos, Vasso, Georgiou, Nikitas, Tzeli, Demeter, Mavromoustakos, Thomas, Moore, Graham J, Kelaidonis, Konstantinos, Matsoukas, Minos-Timotheos, Tsiodras, Sotirios, Swiderski, Jordan, Gadanec, Laura Kate, Zulli, Anthony, Chasapis, Christos T and Matsoukas, John (2024) Density functional theory and enzyme studies support interactions between angiotensin receptor blockers and angiotensin converting enzyme-2: Relevance to coronavirus 2019. Bioorganic Chemistry, 150. ISSN 0045-2068

Bioorganic Chemistry 150 (2024) 107602

Contents lists available at ScienceDirect

Bioorganic Chemistry

journal homepage: www.elsevier.com/locate/bioorg

Density functional theory and enzyme studies support interactions between angiotensin receptor blockers and angiotensin converting enzyme-2: Relevance to coronavirus 2019

Vasso Apostolopoulos [a,b,*], Nikitas Georgiou [c], Demeter Tzeli [d,e,**], Thomas Mavromoustakos [c,***], Graham J. Moore [f,g], Konstantinos Kelaidonis [h], Minos-Timotheos Matsoukas [i], Sotirios Tsiodras [j], Jordan Swiderski [a], Laura Kate Gadanec [a,*], Anthony Zulli [a], Christos T. Chasapis [k,****], John M. Matsoukas [a,g,h,l,*]

[a] Institute for Health and Sport, Victoria University, Melbourne, Victoria 3030, Australia
[b] Immunology Program, Australian Institute for Musculoskeletal Science (AIMSS), Melbourne, Victoria 3021, Australia
[c] Laboratory of Organic Chemistry, Department of Chemistry, National and Kapodistrian University of Athens, Panepistimioupolis Zografou, 11571 Athens, Greece
[d] Laboratory of Physical Chemistry, Department of Chemistry, National and Kapodistrian University of Athens, Panepistimioupolis Zografou, 11571 Athens, Greece
[e] Theoretical and Physical Chemistry Institute, National Hellenic Research Foundation, 48 Vassileos Constantinou Ave., 11635 Athens, Greece
[f] Pepmetics Inc., 772 Murphy Place, Victoria, BC V8Y 3H4, Canada
[g] Department of Physiology and Pharmacology, Cumming School of Medicine, University of Calgary, Calgary, AB T2N 1N4, Canada
[h] NewDrug PC, Patras Science Park, Patras, 26504, Greece
[i] Department of Biomedical Engineering, University of West Attica, Athens 12243, Greece
[j] 4th Department of Internal Medicine, School of Medicine, National and Kapodistrian University of Athens, 11527 Athens, Greece
[k] Institute of Chemical Biology, National Hellenic Research Foundation, 11635 Athens, Greece
[l] Department of Chemistry, University of Patras, Patras, Greece

ARTICLE INFO

Keywords:
Angiotensin-converting enzyme-2
Angiotensin receptor blockers
Coronavirus 2019
Density functional theory
Hypertension
Proton transfer
Severe acute respiratory syndrome coronavirus

ABSTRACT

The binding affinities and interactions between eight drug candidates, both commercially available (candesartan; losartan; losartan carboxylic acid; nirmatrelvir; telmisartan) and newly synthesized benzimidazole-*N*-biphenyltetrazole (ACC519T), benzimidazole bis-N,N'-biphenyltetrazole (ACC519T(2) and 4-butyl-N,*N*-bis([2-(2H-tetrazol-5-yl)biphenyl-4-yl]) methyl (BV6), and the active site of angiotensin-converting enzyme-2 (ACE2) were evaluated for their potential as inhibitors against SARS-CoV-2 and regulators of ACE2 function through Density Functional Theory methodology and enzyme activity assays, respectively. Notably, telmisartan and ACC519T(2) exhibited pronounced binding affinities, forming strong interactions with ACE2′s active center, favorably accepting proton from the guanidinium group of arginine273. The ordering of candidates by binding affinity and reactivity descriptors, emerged as telmisartan > ACC519T(2) > candesartan > ACC519T > losartan carboxylic acid > BV6 > losartan > nirmatrelvir. Proton transfers among the active center amino acids revealed their interconnectedness, highlighting a chain-like proton transfer involving tyrosine, phenylalanine, and histidine. Furthermore, these candidates revealed their potential antiviral abilities by influencing proton transfer within the ACE2 active site. Furthermore, through an *in vitro* pharmacological assays we determined that candesartan and the BV6 derivative, 4-butyl-N,N0-bis[20-2*Htetrazol*-5-*yl*)*bipheyl*-4-*yl*]methyl)imidazolium bromide (BV6 $(K^+)_2$) also contain the capacity to increase ACE2 functional activity. This comprehensive analysis collectively

* Corresponding authors at: Institute for Health and Sport, Victoria University, Melbourne, Victoria 3030, Australia (V. Apostolopoulos, L.K. Gadanec, J.M. Matsoukas).
** Corresponding author at: Laboratory of Physical Chemistry, Department of Chemistry, National and Kapodistrian University of Athens, Panepistimioupolis Zografou, 11571 Athens, Greece (D. Tzeli).
*** Corresponding author at: Laboratory of Organic Chemistry, Department of Chemistry, National and Kapodistrian University of Athens, Panepistimioupolis Zografou, 11571 Athens, Greece (T. Mavromoustakos).
**** Corresponding author at: Institute of Chemical Biology, National Hellenic Research Foundation, 11635 Athens, Greece (C.T. Chasapis).
E-mail addresses: vasso.apostolopoulos@vu.edu.au (V. Apostolopoulos), nikitage@chem.uoa.gr (N. Georgiou), tzeli@chem.uoa.gr (D. Tzeli), tmavrom@chem.uoa.gr (T. Mavromoustakos), mooregj@shaw.ca (G.J. Moore), imats@upatras.gr (M.-T. Matsoukas), jordan.swiderski@live.vu.edu.au (J. Swiderski), laura.gadanec@live.vu.edu.au (L. Kate Gadanec), anthony.zulli@vu.edu.au (A. Zulli), cchasapis@eie.gr (C.T. Chasapis), imats1953@gmail.com (J.M. Matsoukas).

https://doi.org/10.1016/j.bioorg.2024.107602
Received 18 February 2024; Received in revised form 14 June 2024; Accepted 26 June 2024
Available online 28 June 2024

underscores the promise of these compounds as potential therapeutic agents against SARS-CoV-2 by targeting crucial protein interactions.

1. Introduction

The renin-angiotensin system (RAS) is an important hormonal regulatory system responsible for various physiological functions, including systemic blood pressure and fluid homeostasis. Angiotensin II (AngII) is a potent mediator of the RAS, exerting physiological and pathophysiological effects through AngII type 1 receptor (AT1R) signaling to promote vasoconstriction, oxidative stress, fibrosis, and inflammation [1,2]. Angiotensin converting enzyme-2 (ACE2) is a critical component of the RAS, the zinc metallopeptidase is responsible for the hydrolysis of AngII into the heptapeptide angiotensin (1–7) (Ang (1–7)), which subsequently is shown to contain antagonistic effects against the deleterious AngII/AT1R pathways through Mas1 oncogene receptor (MasR) signaling [3]. In various animal models, upregulation of ACE2 and Ang (1–7) activity promotes vasodilation, reduces hypertension and is protective against cardiovascular dysfunction [4–7]. In contrast, ACE2 deficiency is observed to significantly increase circulation of AngII, promote vascular inflammation and oxidative stress [8,9]. RAS dysfunction is believed to play a central role Therefore, these studies suggest the therapeutic potential of increased ACE2 activation against a range of diseases.

The interest in ACE2 occurs beyond its role in the RAS, as ACE2 has been identified as a receptor responsible for the entry of severe acute respiratory syndrome coronavirus 2 (SARS-CoV-2) into host cells [10–12]. SARS-CoV-2 invasion has been reported to downregulate ACE2 expression and its functional enzymatic ability to cleave AngII into Ang (1–7), resulting in an increased AngII-mediated signaling and reduced protective Ang (1–7)/MasR signaling [13,14]. This RAS imbalance is consistent with the clinical conditions of coronavirus 2019 (COVID-19), contributing to hypertension and other cardiovascular pathologies, exacerbated inflammatory response and greater degree of tissue damage in severe cases [15]. Hypertension is a significant condition [16], making the role of ACE2 in viral entry and its therapeutic potential highly important. Consequently, extensive research has focused on developing new antiviral treatments that target ACE2 activation and inhibit the virus's interaction with host ACE2 [17,18].

Sartans are a group of commercially available angiotensin-receptor blockers (ARBs) for the treatment of high blood pressure and other various cardiovascular and renal diseases [19,20]. Multiple observational studies have reported hypertension as one of the most common comorbidities associated with poor clinical outcomes, disease severity and mortality in COVID-19 patients [21]. Due to their ability to inhibit AngII-mediated signaling, sartans have been proposed as therapeutically beneficial in managing COVID-19 by restoring RAS dysfunction and cardiovascular homeostasis [15]. Importantly, hypertensive COVID-19 patients taking ARBs and other medications targeting peptides of the RAS (i.e., ACE inhibitors) have a significantly lower risk of severity and mortality [22,23]. "Bisartans" are a novel family of sartan-like ARBs, which through molecular docking and molecular dynamic simulations we have previously shown to have a strong binding affinity to multiple active sites of ACE2 [24,25]. Recently, we have reported the antiviral abilities of commercially available sartans (i.e., candesartan, losartan and losartan carboxylic acid) and novel bisartans (benzimidazole-*N*-biphenyl (ACC519C) and benzimidazole-*N*-biphenyltetrazole (ACC519T)d) in comparison to nirmatrelvir (antiviral component in Pfizer's paxlovid) against SARS-CoV-2 in cell studies [26]. In this study, we demonstrated the abilities of sartans and bisartans to interact with the amino acid residues in the ACE2/S protein receptor binding domain (RBD) complex, resulting in candesartan and ACC519C having equipotent antiviral effects to nirmatrelvir (95 % inhibition of viral cytopathic effect), followed by ACC519T (85 %) and losartan (80 %) while losartan carboxylic was least effective (50 %) [26].

In this study, we investigated the binding affinity of eight drugs, both commercially available (i.e., candesartan, losartan, losartan carboxylic acid, nirmatrelvir, and telmisartan) and newly synthesized (i.e., ACC519T, benzimidazole bis-N,N'-biphenyltetrazole (ACC519T(2)), and 4-butyl-N,*N*-bis([2-(2H-tetrazol-5-yl)biphenyl-4-yl]) methyl (BV6)), to the active site of ACE2. This was achieved using Density Functional Theory (DFT), a precise quantum–mechanical-mechanical method for calculating the electronic structure of molecular systems [27]. Prompted by these results, we also investigated the ability of these molecules to modulate the catalytic activity of ACE2 through *in vitro* enzymatic assay.

This study aims to provide a detailed examination of the binding interactions between these molecules and the amino acids at the active site of ACE2, using a combination of *in silico* and experimental approaches. Additionally, we calculate their reactivity descriptors to identify the most promising candidates for preventing SARS-CoV-2 infection. Docking calculations revealed proton (H^+) transfer in some of these bisartans to the arginine (Arg) amino acid, and it was discovered that AngII might have a charge relay system involving three amino acids: tyrosine, histidine, and phenylalanine [24,25,28]. The present study provides synthetic organic and bioorganic chemistry with useful information about the binding activity of sartans and bisartans to develop dual-activity drug candidates that contain significant antiviral, antihypertensive and cardiovascular protective effects.

2. Materials and methods

2.1. Computational details

The binding affinities of the experimental drugs (i.e., ACC519T, ACC519T(2), BV6, candesartan, losartan, losartan carboxylic acid, nirmatrelvir and telmisartan) to the active site of ACE2 were calculated using the DFT at the B3LYP/6–311 + G(d,p) level of theory, which has been regarded as an appropriate calculation for the present molecular systems [29–31]. The ligands were positioned within the binding site based on the results obtained from molecular docking studies and the geometries were further optimized. The interaction between the drugs and the three amino acids of the ACE2 active site (i.e., Arg273, tryptophan (Trp) 271 and aspartic acid (Asp) 269) were calculated and are represented in Fig. 1. The highest occupied molecular orbitals (HOMO) and the lowest unoccupied molecular orbitals (LUMO) of the free dugs and of the interacted drugs with the previously mentioned amino acids were plotted (Figs. 1S–16S). Various reactivity descriptors and properties related to the chemical reactivity of drugs, including HOMO-LUMO (H-L) gap, ionization potential (IP) and electron affinity (EA), electronegativity ($\chi = (IP + EA)/2$), chemical hardness ($\eta = (IP - EA)/2$), chemical potential ($\mu = -\chi$), and electrophilicity index ($\omega = \mu^2/2\eta$) were also calculated for the free and encapsulated drugs [32], where small deformations are observed in their geometries due to interactions with the active site of ACE2. Note that IP and EA values were calculated using Koopman's theory according to which IP is regarded as $-E_{HOMO}$ and EA as $-E_{LUMO}$. Finally, the charges of the N atoms of the drugs that accept H^+ from the guanidinium group of ARG273 were calculated using the Mulliken and Hirshfeld charge model 5 (CM5) population analyses [33].

The H^+ transfer in the tyrosine (Tyr)-histidine (His) and His-phenylalanine (Phe) peptide dimer and in the Tyr-His-Phe peptide trimer which are included in ACE2 receptor was calculated using DFT (B3LYP/6–311 + G(d,p)) methodology. The amino acids and their deprotonated analogues, the peptide dimers and trimer were optimized using B3LYP/6–311 + G(d,p) to find the lowest in energy minimum structures. The transition states for the proton transfer in peptide dimers

and trimer were also calculated. All the calculations were performed in water solvent employing the polarizable continuum model (PCM) [34]. All calculations and visualizations in this experiment were carried out using Gaussian 16 [35].

2.2. In vitro ACE2 activity assay

ACE2 enzyme assays were carried out in a total volume of 2 mL, containing a final concentration of 50 ng/mL recombinant human ACE2 (rhACE2) (Cat#933ZN010; R & D systems, Oxford, UK) dissolved in a buffer solution consisting of 50 mM HEPEs (Cat#H3375; Sigma Aldrich, MO, USA), 100 mM NaCl (Cat#S9888; Sigma Aldrich, MO, USA), and 10 μM zinc acetate (Cat#CM2750; Ajax Chemicals, NSW, AU) (pH 7.0) [36–38]. To assess the effects of sartans on rhACE2 activity, samples (n = 5) were left alone (positive control) or pre-incubated with 1 μM of candesartan (Cat#SML0245; Sigma Aldrich, MO, USA), telmisartan (Cat#S1738; Selleck Chemicals, TX, USA), nirmatrelvir (Cat#-AOB14800; Aobious, MA, USA), ACC519T, ACC519T(2), or BV6(K^+)$_2$ for 10 min at 37 °C. To initiate the reaction, 100 μM AngII was added, and the sample was immediately vortexed and incubated at 37 °C for 60 min [18]. Samples without AngII served as the negative control. The reaction was stopped by placing the samples in an 80 °C water bath for 5 min to denature the enzyme, after which samples were placed on ice. The resulting samples were transferred into an injection vial and the catalysis of AngII into Ang(1–7) by ACE2 was determined by high performance liquid chromatography (HPLC) analysis performed on a series LC-2030 HPLC-UV (Shimadzu Corporation, Japan) using a Kinetex® C18 100A^o reverse-phase LC column (5 μM, 250 × 4.6 mm) with a UV detector set a 220 nM. Peptide separations were carried out at room temperature at a flow rate of 0.4 mL/min. Mobile A consisted of MiliQ with 0.1 % formic acid (Cat#543804; Sigma Aldrich, MO, USA), and mobile B consisted of HPLC grade acetonitrile (Cat#543804; Sigma Aldrich, MO, USA) and 0.1 % formic acid. A linear solvent gradient of 10–70 % B, over 9 min, 70–10 % over 2 min, and a final 4 min at the final concentration with a 10-minute re-equilibration period was used. Identification of peptides and their quantification was based upon the elution time of known amounts of synthetic AngII (Cat#51480; Mimotopes, VIC, AUS) and Ang (1–7) (Cat#A14862; AdooQ Bioscience, CA, USA) standards.

Using the same protocol as above, a dose–response curve for candesartan and BV6(K^+)$_2$ was performed in triplicate by incubating rhACE2 with or without the presence of titrating concentrations of 10^{-12}–10^{-6} M candesartan or BV6(K^+)$_2$. The dose–response curve was constructed by plotting the % of ACE2 activity without the presence of sartan incubation and the log concentration of sartans.

2.3. Statistical analysis

Data represented as mean ± standard error of mean (SEM) with n representing the number of samples. GraphPad prism (Version 10) was utilized for graphical representation and statistical analysis of ACE2 activity. Statistical analysis was performed using a one-way analysis of variance (ANOVA) followed by Dunnett's post-hoc test to compare effect of sartan on ACE2 activity compared to positive control while a two-way ANOVA followed by Sidak's post-hoc test was performed to compare the dose–response between candesartan and BV6(K^+)$_2$. The value of $p < 0.05$ was considered statistically significant.

3. Results

3.1. Interaction of sartans with the active center of ACE2 computational details

The minimum energy structures of the eight experimental drugs are shown in Fig. 2. Furthermore, the interactions between the active site of ACE2 and these experimental drugs were analyzed, revealing that an H^+ cation was transferred from the guanidinium group of Arg273 to a nitrogen atom of the drug. In all instances, this transfer occurred without an energy gap, as illustrated in Fig. 3. The system is more stable having the H^+ atom connected to the drug than to Arg273 and both Mulliken and CM5 predict similar charges. Moreover, it is found that the benzimidazole group has a greater negatively charged N atom that accepts H^+ in tetrazole, resulting in H^+ acceptance from the guanidinium group of Arg273, while the N atom of candesartan and losartan acid are less nucleophile atoms, as shown in Table 1.

The frontiers molecular orbitals (HOMO and LUMO) of the free drugs and of the complex molecular systems consisting of the drug and the interacting amino acids, (i.e., Arg273, Trp271 and Asp269) are depicted in Fig. 4. In all cases, but telmisartan, the HOMO is located on Trp271, while the LUMO in the drug, showing that the lowest in energy electron transfer is an intermolecular process. Thus, at first the drug accepts an H^+ from the guanidinium group of Arg273 and then it may also accept an electron from Trp271 given that the necessary energy requirements are fulfilled.

Several reactivity descriptors of the above drugs were calculated for the free drugs and for the drugs interacting with the amino acids, where small deformations are observed in their geometries due to the interactions with the active center of the ACE2. Specifically, H–L gap, electronegativity, chemical hardness, chemical potential, electrophilicity index and binding energy (kcal/mol) were calculated for each drug and are shown in Table 2. The larger the H-L gap, the more excitation

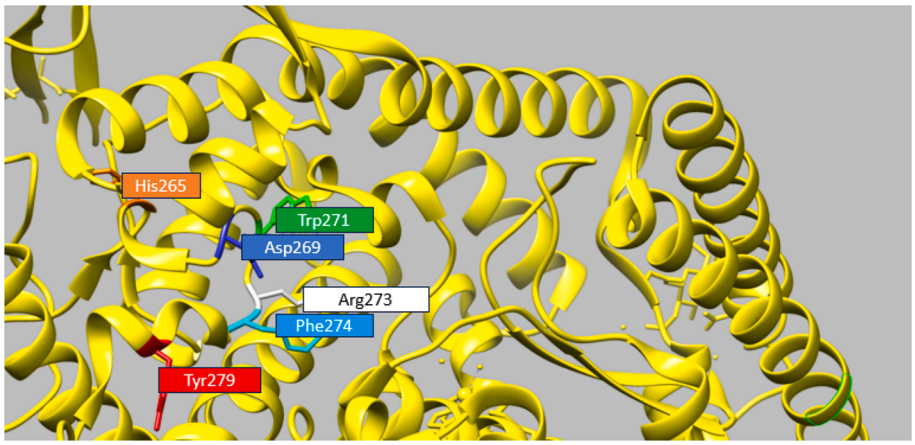

Fig. 1. Active site of ACE2. *Abbreviations:* ACE2, angiotensin-converting enzyme-2; Arg, arginine (white); Asp, aspartic acid (blue); His, histidine (orange); Phe, phenylalanine (cyan); Trp, tryptophan (green); Tyr, tyrosine (red). (For interpretation of the references to colour in this figure legend, the reader is referred to the web version of this article.)

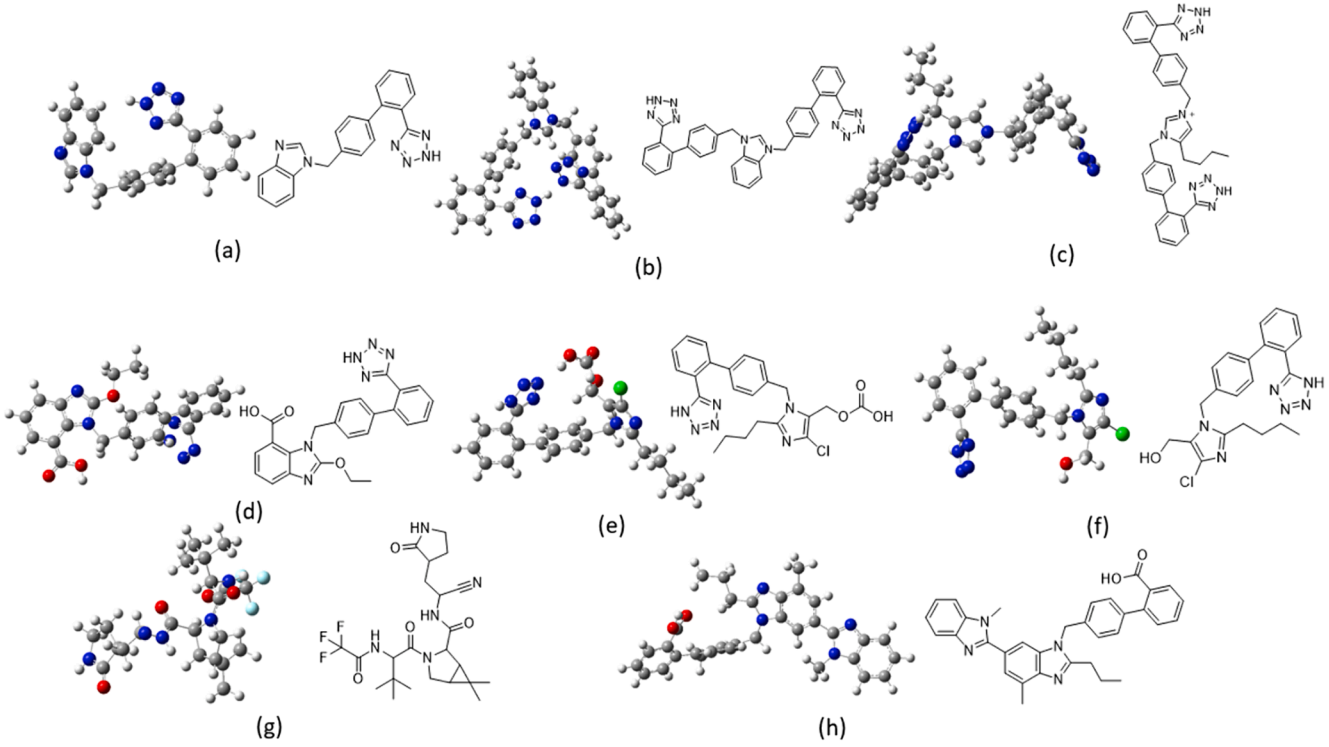

Fig. 2. 2D and 3D structures of (a) ACC519T, (b) ACC519T(2), (c) BV6, (d) candesartan, (e) losartan carboxylic acid, (f) losartan, (g) nirmatrelvir (g) and (h) telmisartan. *Abbreviations:* ACC519, benzimidazole-*N*-biphenyltetrazole; ACC519T(2), benzimidazole bis-N,N'-biphenyltetrazole; BV6, 4-butyl-N,N-bis[2-(2H-tetrazol-5-yl)biphenyl-4-yl] methyl.

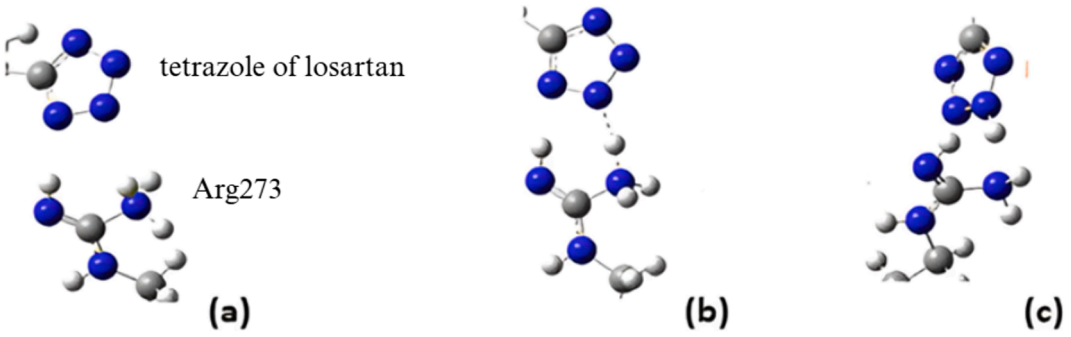

Fig. 3. H^+-transfer from the guanidinium group of ARG273 to losartan. (a) Interactions between losartan tetrazole and ARG273 segment, (b) transfer of H^+ from ARG273 to nitrogen of losartan tetrazole (c) Transfer or H^+ from ARG273 to tetrazole of losartan. *Abbreviations:* ARG, arginine; H^+, proton.

energy is needed for electron transfer. The large H-L gap, and thus the large chemical hardness, is an indication of an increased stability. On the contrary, a small energy gap indicates high chemical reactivity. Thus, the free nirmatrelvir has the highest H-L gap indicating stability with respect to an electron transfer. The ordering from the highest H-L gap to the lowest is nirmatrelvir > ACC519T > BV6 ≥ losartan > losartan carboxylic acid > candesartan ≥ ACC519T(2) > telmisartan and the telmisartan presents the highest reactivity (Table 2). When the drugs interact with the amino acids, the ordering of the H-L gap of the drugs changes to nirmatrelvir > ACC519T(2) > losartan carboxylic acid > ACC519T > losartan ≥ candesartan > BV6 > telmisartan (Table 2); however, both nirmatrelvir and telmisartan also have the highest and lowest H-L, respectively. Considering the complex as a whole system, the ordering is ACC519T ≥ losartan > ACC519T(2) ≥ BV6 ≥ nirmatrelvir > candesartan > losartan carboxylic acid > telmisartan (Table 2).

Chemical potential indicates the escape from a stable system. It has been reported that as chemical potential decreases, the reactivity of a species increases. Therefore, the most reactive compound in our study is the benzimidazole in ACC519T(2), whereas nirmatrelvir is the least reactive. The electrophilicity index (ω) is a crucial reactivity descriptor that helps in understanding the reactivity of chemical species, representing a system's ability to accept electrons. A low electrophilicity index indicates good nucleophilicity, while a high value signifies strong electrophilic behaviour. Thus, nirmatrelvir is the superior nucleophile, while telmisartan is the superior electrophile (Table 2). Regarding the binding energy of the drugs with the three amino acids, the binding energies are larger than in the complex of receptor binding domain (RBD) of SARS-CoV-2 and ACE; however, the ordering remains almost the same, telmisartan > ACC519T(2) > candesartan > ACC519T > losartan carboxylic acid > BV6 > losartan > nirmatrelvir which is characteristic of the binding ability of the drugs (Table 2). Therefore, telmisartan and ACC519T(2) have stronger binding with the active centre of ACE2, as well as displaying the most negatively charged N atoms in tetrazole that accept H^+, showing that hydrogen cation of the guanidinium group of Arg273 can more easily be accepted.

Table 1
CM5 charges[a] on N atoms of Arg273 N (+) and N═ (double bond) and N (−) at the lowest in energy optimized molecular systems of the drug compound interacting with Arg273, Trp271 Asp269.

Drugs	N (+)	N (−)	N═
Losartan	−0.01	−0.10	−0.28
ACC519T	−0.02	−0.31	−0.20
ACC519T(2)	0.02	−0.22	−0.29
BV6	−0.03	−0.19	−0.31
Candesartan	0.02	0.20	−0.31
Losartan[b]	0.37	−0.14	−0.27
Losartan[c]	0.42	−0.16	−0.22
Losartan acid	0.05	0.18	−0.31
Nirmatrelvir	0.45		−0.24
Telmisartan	−0.01	−0.06	−0.33

[a] Hydrogens bonded to nitrogen atoms are summed into N atoms.
[b] Transition state for the H^+ atom transfer from arginine to drug.
[c] Minimum structure with H^+ atom attached to arginine. *Abbreviations:* ACC519, benzimidazole-*N*-biphenyltetrazole; ACC519T(2), benzimidazole bis-N,N'-biphenyltetrazole; Arg, arginine; Asp, aspartic acid; BV6, 4-butyl-N,N-bis [2-(2H-tetrazol-5-yl)biphenyl-4-yl] methyl; CM5, charge model 5; H^+, hydrogen; N, nitrogen; Trp, tryptophan.

3.2. H^+ transfer in tyrosine-histidine-phenylalanine of ACE2 receptor

The H^+ transfer among the amino acids of the active center in ACE2 receptor, where the drug binds (i.e., tyrosine (Tyr) 41, phenylalanine (Phe) 40, and histidine (His) 34), were studied and are presented in Fig. 5. Proton transfer in the Tyr-His-Phe system was also examined, which occurs in the AngII active site [39]. The lowest energy conformations of Tyr, His, and Phe were calculated along with their peptide dimers and the peptide trimer systems. Proton transfer in Tyr41-His34 (Tyr-H…His-H) and His34-Phe40 (His-H…Phe) were calculated, as well as the corresponding H^+ transfer from Tyr41 to the N atom of His34 to the carboxylate group of Phe40. The H^+ transfer was examined in the corresponding Tyr-His-Phe system (Figs. 5 and 6).

The H bond distances of dimers and trimers are provided in Table 3 for all minimum energy structures and transition states. The N—H covalent bond distances range from 1.0 to 1.1 Å, with corresponding bond distances in transition states around 1.3 Å. The N…H van der Waals distances range from 1.4 to 1.6 Å. The formed O—H covalent bond is approximately 1.06 Å, and the corresponding bond distances in transition states are about 1.3 Å. The O…H van der Waals distances are around 1.7 Å. Notably, in transition states, distances NN between Tyr and His and distances NO between His and Phe are reduced by about 0.2 Å, indicating the closer approach of amino acids due to transferred H^+ cations.

It was noted that the proton transfer between two peptides is not

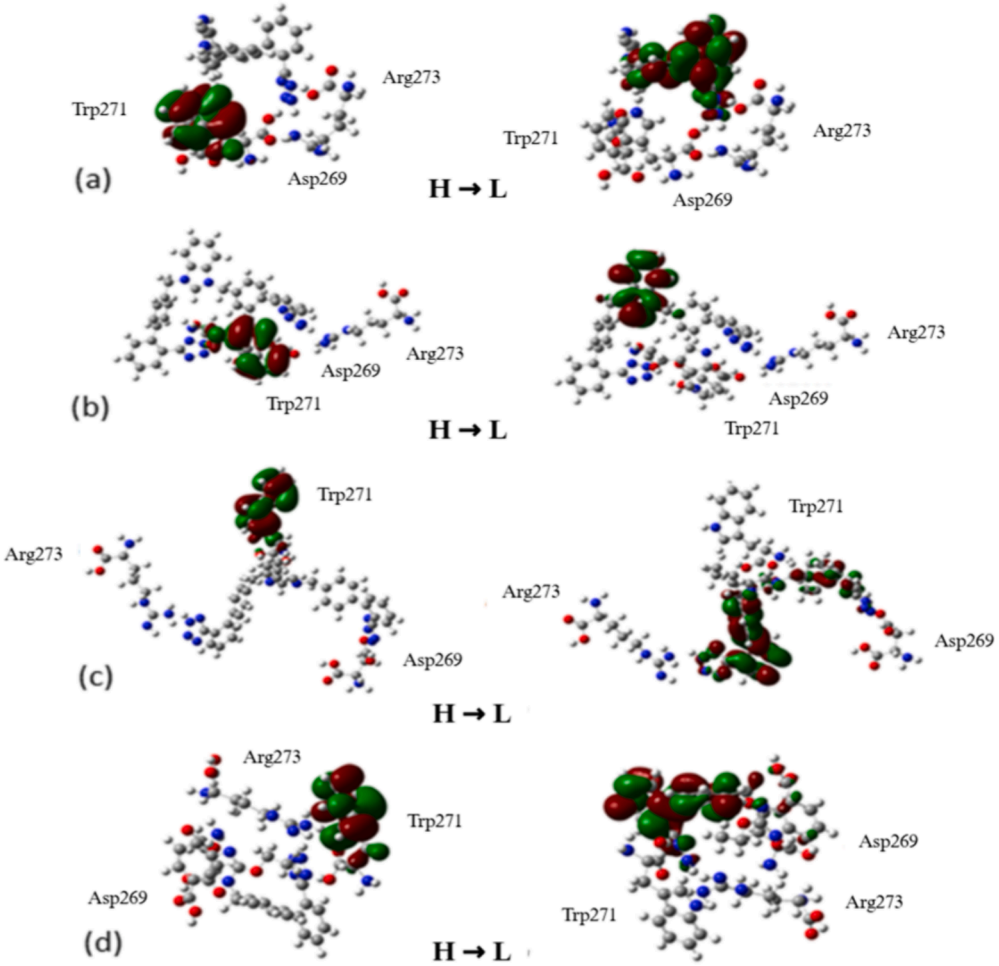

Fig. 4. HOMO and LUMO orbitals of the interacting system of (a) ACC519T, (b) ACC519T(2), (c) BV6, (d) candesartan, (e) losartan, (f) losartan carboxylic acid, (g) nirmatrelvir and (h) telmisartan compound interacting with ARG273, TRP271 and ASP269**.** *Abbreviations:* ACC519, benzimidazole-*N*-biphenyltetrazole; ACC519T(2), benzimidazole bis-N,N'-biphenyltetrazole; ACE2, angiotensin-converting enzyme-2; ARG, arginine; ASP, aspartic acid position; BV6, 4-butyl-N,N-bis{[2-(2H-tetrazol-5-yl)biphenyl-4-yl] methyl; HOMO, highest occupied molecular orbitals; LUMO, lowest unoccupied molecular orbitals; TRP, tryptophan.

Table 2
Reactivity descriptors of the studied drugs, as free drugs, as a part of the complex and of the complex system drug interacting with Arg273, Trp271 and Asp269.

	Free drugs					Interacting drug					Complex					BE
Drugs	H-L	χ	η	μ	ω	H-L	χ	η	μ	ω	H-L	χ	η	μ	ω	
Benzimidazole bis-N,N′ biphenyltetrazole	3.69	4.25	1.85	4.25	4.90	5.01	1.05	2.50	1.05	0.22	4.09	3.47	2.04	3.47	2.94	−32.3
Telmisartan	0.61	3.80	0.31	3.80	23.58	0.61	5.61	0.30	5.61	51.71	0.60	5.42	0.30	5.42	48.65	−34.9
Candesartan	3.72	3.76	1.86	3.76	3.81	4.63	3.87	2.32	3.87	3.23	3.75	3.65	1.88	3.65	3.56	−30.9
Losartan carboxylic acid	3.96	4.14	1.98	4.14	4.32	4.87	4.07	2.43	4.07	3.40	2.84	3.12	1.42	3.12	3.43	−27.4
benzimidazole-*N*-biphenyltetrazole	5.11	3.88	2.55	3.88	2.94	4.70	3.88	2.35	3.88	3.20	4.29	3.79	2.15	3.79	3.35	−29.1
Losartan	4.41	3.98	2.20	3.98	3.60	4.64	3.87	2.32	3.87	3.22	4.22	3.55	2.11	3.55	2.98	−19.2, −11.3, −10.8[a]
Nirmatrelvir	6.17	3.74	3.09	3.74	2.27	5.80	3.78	2.90	3.78	2.46	4.02	5.42	2.01	5.42	7.32	−8.7
BV6	4.47	6.40	2.23	6.40	9.17	4.22	6.62	2.11	6.62	10.38	4.05	5.63	2.02	5.63	7.83	−24.1

[a] Three and two minimum structures. *Abbreviations:* ACC519, benzimidazole-*N*-biphenyltetrazole; ACC519T(2), benzimidazole bis-N,N′-biphenyltetrazole; Arg, arginine; Asp, aspartic acid position; BE, binding energy; BV6, 4-butyl-N,N-bis{[2-(2H-tetrazol-5-yl)biphenyl-4-yl] methyl; Trp, tryptophan; χ, electronegativity; η, chemical hardness; μ, chemical potential; ω; electrophilicity index.

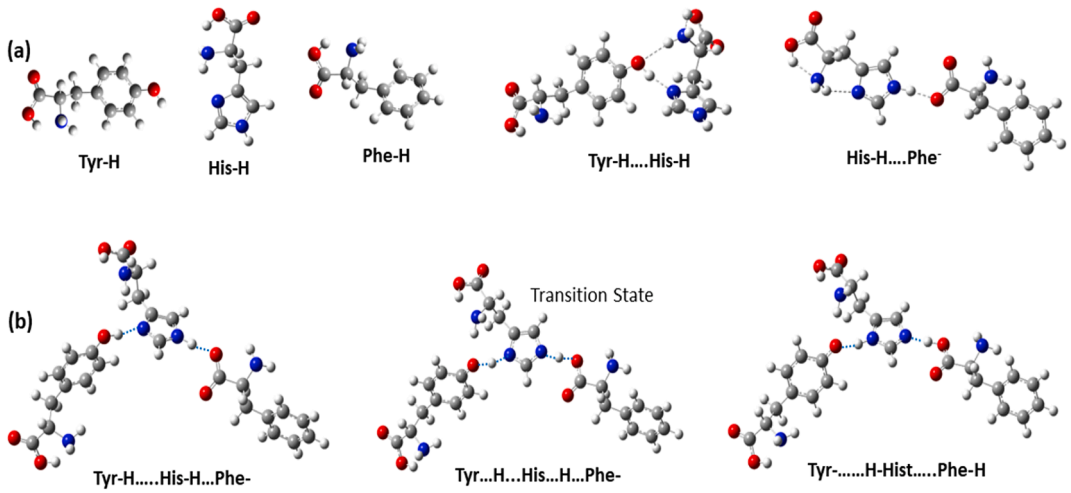

Fig. 5. (a) Calculated minimum energy structures of Tyr41, His34, Phe40 and dimers (b) calculated minimum energy structures of two minima and the corresponding transition state for the H^+ transfer in water solvent using B3LYP/6–311 g(d,p). *Abbreviations:* His, histidine; His-H…Phe; histidine34-phenylalanine40; Phe, phenylalanine; Tyr, tyrosine; Try-H…His-H, tyrosine41-histidine34.

favored. Energetically, the corresponding transition states are almost energetically degenerated with the corresponding products. The potential energy surfaces of hydrogen transfer are very shallow. The shorter hydrogen bonds in the dimers further stabilize the transition states. Thus, even if the proton is transferred, it returns to its original amino acid. The binding energy of the two peptides are −7.59 kcal/mol (Tyr-H…His-H) and −9.12 kcal/mol (His-H…Phe^-), see Table 4. On the contrary, in the peptide trimer, the proton transfer can occur. At first, the proton is transferred from Tyr-H to His-H via the Tyr….H…. His-H…. Phe^- transition state and then the second H^+ is transferred via the Tyr….H….His…H….Phe^- transition state. The energetic demands are very small, i.e., 3.6 kcal/mol and additional 2.9 kcal/mol, as shown in see Fig. 7. The binding energy of the Tyr-H…His-H…Phe^- and Tyr^-…H-His…Phe-H complexes with respect to the corresponding involved monomer species are −16.15 and −29.29 kcal/mol, respectively. These binding energy values show that even though the Tyr^-…H-His…Phe-H complex is 5.1 kcal/mol, higher than the Tyr-H…His-H…Phe^- complex, its BE is 13.2 kcal/mol larger than the binding energy of Tyr-H…His-H…Phe^- complex, see Fig. 8.

The IR spectra of the Tyr-H…His-H…Phe^- and Tyr^-…H-His…Phe-H complexes are depicted in Fig. 8. Both are true minima, i.e., there are not any imaginary frequencies. Their first normal mode frequency is only 4 cm^{-1}, and it corresponds to a bend motion of the peptide trimer. The normal mode frequencies that correspond to the stretching of the covalent hydrogen bond, which breaks and the H^+ is transferred from one amino acid to another are given in Table 4. It is found that in both minima, the H bond stretching of Tyr-H-His is higher in energy than the H bond stretching of His-H-Phe. Furthermore, in the Tyr-H…His-H…Phe^- trimer, the normal modes are higher in energy than in Tyr^-…H-His…Phe-H as shown in Fig. 7 that larger energy is required for proton transfer in the first complex than in the second one. However, even for the higher in energy normal mode of H covalent bond stretching of 3039 cm^{-1} (=8.69 kcal/mol), the energy demand is covered energetically by the binding energy of the Tyr^-…H-His…Phe-H.

3.3. Determination of rhACE2 enzyme activity

In order to investigate the effects of these compounds on ACE2 catalytic activity, sartans were incubated with rhACE2 in the presence of AngII to measure its degradation and conversion to Ang(1–7). Incubation of ACC519T, ACC519T(2), telmisartan, and nirmatrelvir had no significant effect on rhACE2 activity. Interestingly, incubation of candesartan and the novel BV6 derivative, $BV6(K^+)_2$, increased activity of rhACE2, as shown by the significant reduction of AngII and subsequent increase in Ang(1–7) when compared to the positive control group (Table 5, Fig. 9A and B). Candesartan and $BV6(K^+)_2$ both displayed a

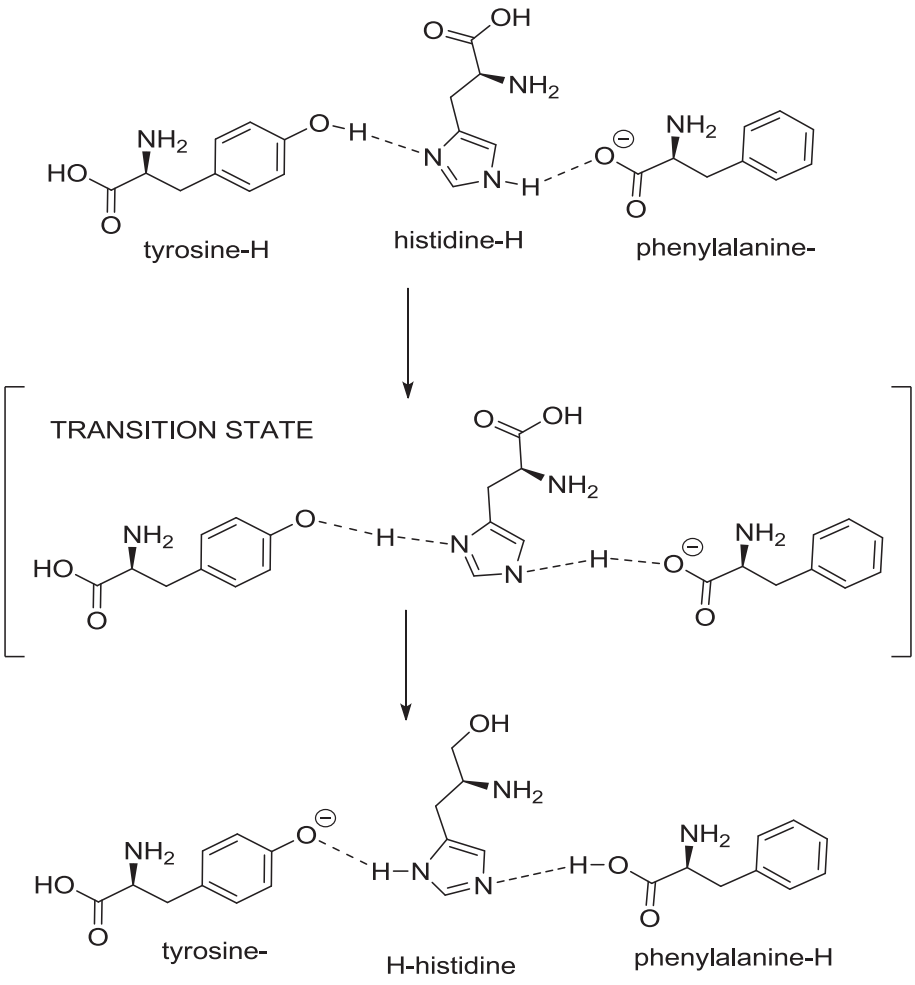

Fig. 6. H^+ transfer in the tyrosine-histidine-phenylalanine peptides.

Table 3
Selected hydrogen bond distances R(Å) and angles θ(degrees) involved in the proton transfer of the minima (m) and transition states (ts) and relative energies T_e (kcal/mol) in water solvent at B3LYP/6–311 g(d,p).

		R_{OH}	R_{HN}	θ_{OHN}	R_{NH}	R_{HO}	θ_{NHO}	T_e
Tyr-H….His-H	m	1.004	1.717	167.6				0.00
Tyr…H….His-H	TS	1.294	1.189	171.2				6.93
Tyr…H-His-H	m	1.361	1.139	169.7				7.28
His-H….Phe^-	m				1.049	1.685	175.1	0.00
His…H….Phe^-	TS				1.106	1.302	176.4	6.89
His^-…H-Phe	m				1.504	1.063	173.7	8.83
Tyr-H….His-H….Phe^-	m	1.002	1.736	172.7	1.053	1.662	175.3	0.00
Tyr….H….His-H….Phe^-	TS	1.354	1.159	169.7	1.069	1.592	178.4	3.56
Tyr….H….His…H….Phe^-	TS	1.313	1.240	167.1	1.207	1.335	175.8	6.52
Tyr^-….H-His…H-Phe	m	1.593	1.065	166.9	1.546	1.054	175.5	5.12

dose-dependent increase in ACE2 activity with $BV6(K^+)_2$ displaying a significantly greater ability to increase ACE2 activity than candesartan at concentrations of [10^{-9} M] ($p < 0.001$) to [10^{-6} M] ($p < 0.001$)and 2.7-fold higher potency with an EC_{50} of 9.63 nM vs 26.2 nM, respectively (Fig. 10).

4. Discussion

Based on losartan and our Charge Relay System conformational model for AngII, we have designed and synthesized another class of sartans called elsartans [39–41]. Furthermore, bisartans [42] provide significant advances in drug discovery of new antihypertensives. Elsartans were designed based on losartan by rotation of the butyl and hydroxy methylene group at positions 2 and 4 of the imidazole group and differed to all known sartans by having lipophilic butyl group at position 4. Elsartans are efficiently synthesized and are superior in potency compared to losartan [38]. Bisartans, built on imidazole scaffold, bear two biphenyl tetrazole groups as warheads attached on the two nitrogen's of the scaffold aromatic ring were found to be stronger binders to ACE2 by computational and enzyme methods compared to known sartans [39–41]. A recent study (unpublished results), by equilibrium molecular dynamics methods, has shown benzimidazole based bisartan ACC519T(2) to be a strong binder to furin which cleaves SARS-CoV-2 spike protein at arginine rich sequences S1/S2 and S2́ initiating infection. In all these studies Arg has been found to play a dominant role in mutations and infectivity [43,44] and tetrazole to be a strong binder.

Table 4
BE (kcal/mol) selected normal modes ω (cm^{-1}) and relative energies T_e (kcal/mol) of the dimers and trimers minima in water solvent at B3LYP/6–311 g(d,p).

	Tyr-H…His-H	Hist-H…Phe$^-$
BE	−7.59	−9.12
	Tyr-H…His-H…Phe$^-$	**Tyr$^-$…H-His…Phe-H**
BE	−16.15	−29.29
ω_1	4.0	4.0
ω (H-bond stretching, Tyr-H-His)	2838	2162
ω (H-bond stretching, His-H-Phe)	3039	2641
T_e (electronic)	0	5.12
T_e (electronic + ZPE[a])	0	4.27
T_e (Gibbs Free Energy)	0	5.52

[a] ZPE: Zero-point energy. *Abbreviations:* BE, binding energy; His-H…Phe; histidine34-phenylalanine40; Te, relative energies; Try-H…His-H, tyrosine41-histidine34.

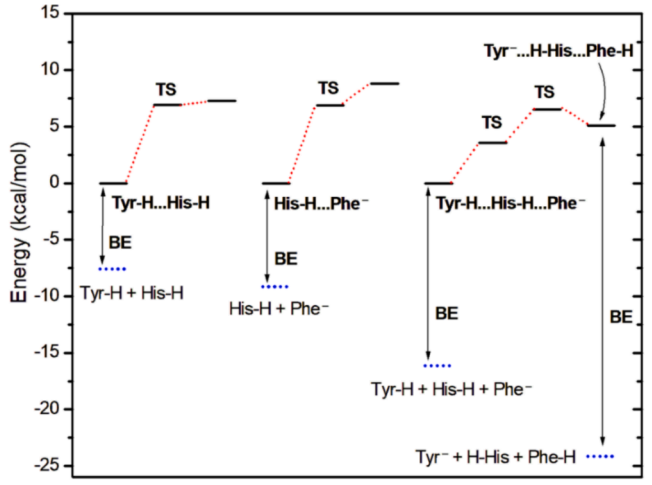

Fig. 7. Reaction energy path of the H^+ transfer in Tyr-His and His-Phe and in Tyr-His-Phe.

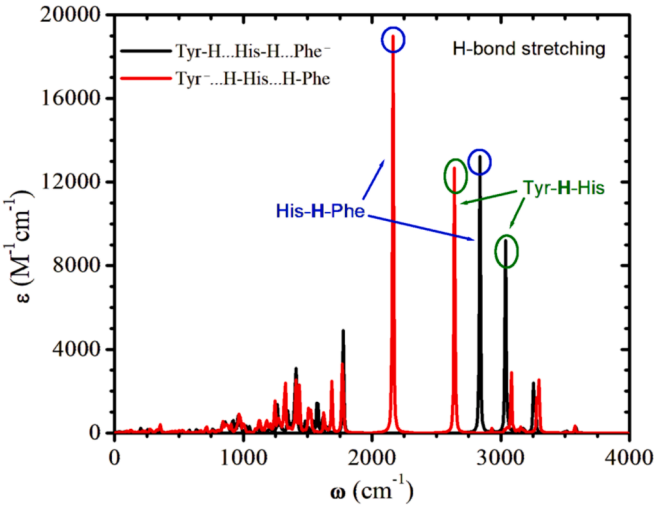

Fig. 8. IR Spectra of the Tyr-H…His-H…Phe$^-$ and Tyr$^-$…H-His…Phe-H minima.

Other physical chemistry methods like crystallography and nuclear magnetic resonance, specifically two-dimensional NMR techniques, are available in the armament of drug discovery to identify predicted interactions between ligand and protease receptors as well between inter and intra interacting residues.

Table 5
Effect of sartan incubation with rhACE2 to determine changes in metabolism of AngII.

Drug	AngII	Ang (1–7)
	Mean ± SEM (μM)	Mean ± SEM (μM)
Negative Control	100.9 ± 0.45	N/A
Positive Control	98.5 ± 0.47	1.002 ± 0.05
Candesartan	95.7 ± 0.49	1.38 ± 0.05
Telmisartan	98.6 ± 0.54	1.04 ± 0.06
Nirmatrelvir	99.5 ± 0.5	0.84 ± 0.03
ACC519T	97.5 ± 1.1	1.08 ± 0.04
ACC519T(2)	97.2 ± 0.55	1.14 ± 0.03
$BV6(K^+)_2$	93.1 ± 0.65	1.64 ± 0.07

In the present study, we report the binding affinities of eight drugs, ACC519T, ACC519T(2), BV6, losartan, losartan carboxylic acid, candesartan, nirmatrelvir, and telmisartan, with the three amino acids of the activate site of ACE2 to determine the best candidates that may prevent SARS-CoV-2 infection. The frontiers molecular orbitals (HOMO and LUMO) of the free drugs and of the complex molecular systems consisting of the drug and the interacting amino acids (i.e., Arg273, Trp271 and Arg269 are depicted in Fig. 4 for the ACC519T and Fig. 1S-8S of the SI for all used drugs. In all cases, but telmisartan, the HOMO is located on Trp271, while the LUMO in the drug, showing that the lowest in energy electron transfer is an intermolecular process. Thus, at first the drug accepts an H^+ from the guanidinium group of Arg273 and then it may also accept an electron from Trp271 given that are the necessary energy requirements. It is of note that in the ACE2 active center, next to the critical Arg273 is residue Phe274, which may positively affect the transfer of an H^+ from the guanidinium group of Arg273 to the drug. This effect is possible through pi-pi interactions between the two side chains of Phe and Arg residues, rich in pi electrons. Previous studies have shown the importance of the Phe/Arg relative conformation for maximum activity [26,45].

Several reactivity descriptors of above drugs were calculated for the free drugs and for the drugs interacting with the amino acids, where small deformations are observed in their geometries due to the interactions with the active center of the ACE2, see Table 2. Specifically, H–L gap, electronegativity χ, chemical hardness η, chemical potential μ, and electrophilicity index ω. The larger the H-L gap, the more excitation energy is needed for an electron transfer. The large H-L gap, and thus the large chemical hardness, is an indication of increased stability. On the contrary, a small energy gap indicates high chemical reactivity. Thus, the free nirmatrelvir, the Pfizer drug, presents the highest H-L gap indicating stability with respect to an electron transfer. The ordering from the highest H-L gap to the lowest is nirmatrelvir > ACC519T > BV6 > losartan > losartan carboxylic acid > candesartan > ACC519T(2) > telmisartan and the telmisartan presents the highest reactivity. When the drugs interact with the amino acids, the ordering of the H-L gap of the drugs changes to nirmatrelvir > ACC519T(2) > losartan carboxylic acid > ACC519T > losartan > candesartan > BV6 > telmisartan; however, both nirmatrelvir and telmisartan also present the highest and the lowest H-L, respectively. Considering the complex as a whole system, the ordering is ACC519T > losartan > ACC519T(2) > BV6 > nirmatrelvir > candesartan > losartan carboxylic acid > telmisartan (Table 2). Chemical potential presents the escaping tendency of electrons involved in a stable system. It is reported that with decreasing chemical potential, the reactivity of species tends to increase. Thus, the most reactive is the ACC519T(2), while the least reactive is nirmatrelvir. The electrophilicity index ω is an important reactivity descriptor that plays a vital role in understanding the reactivity of chemical species as it refers to the capacity of a system to accept electrons. A low value of the electrophilicity index suggests the good nucleophilicity of a compound, while a high value is a sign of good electrophile behavior. Thus, nirmatrelvir is

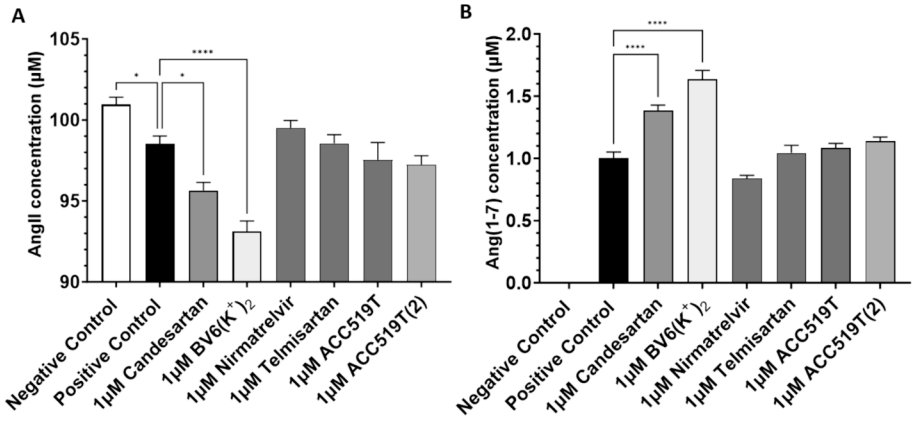

Fig. 9. Retrieved (A) AngII and (B) Ang (1–7) concentration (μM) as a result of AngII metabolism by 50 ng/mL rhACE2 in and without the presence of 1 μM candesartan, telmisartan, nirmatrelvir, ACC519T, ACC519T(2), and BV6(K^+)$_2$. Candesartan (* $p < 0.05$ and **** $p < 0.0001$) and BV6(K^+)$_2$ (**** $p < 0.0001$ and **** $p < 0.0001$) significantly increased rhACE2 metabolism of AngII and production of Ang (1–7) vs. positive control. *Abbreviations*: ACC519, benzimidazole-*N*-biphenyltetrazole; ACC519T(2), benzimidazole bis-N,N′-biphenyltetrazole rhACE2, recombinant human angiotensin converting enzyme 2; BV6(K^+)$_2$, (4-butyl-N,N0-bis[20-2*Htetrazol*-5-*yl)bipheyl*-4-*yl*]methyl)imidazolium bromide); AngII, angiotensin II, Ang (1–7), angiotensin (1–7), SEM, standard error of mean.

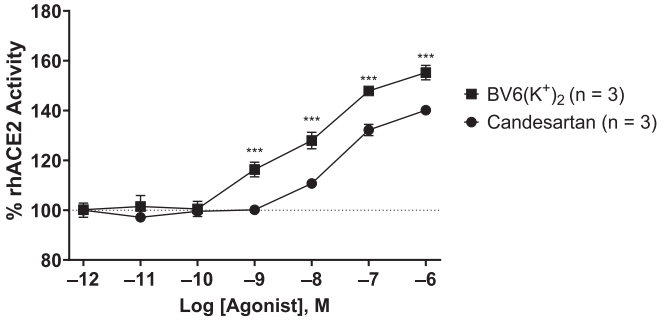

Fig. 10. Activation dose–response curve for rhACE2 metabolism of AngII into Ang (1–7) by increasing concentrations of candesartan and BV6(K^+)$_2$. The EC50 for ACE2 activation by candesartan and BV6(K^+)$_2$ is −7.582 M (26.2 nM) and −8.016 M (9.63 nM), respectively. Abbreviations: rhACE2, recombinant humane angiotensin converting enzyme 2; BV6(K^+)$_2$, (4-butyl-N,N0-bis[20-2*Htetrazol*-5-*yl)bipheyl*-4-*yl*]methyl)imidazolium bromide); AngII, angiotensin II, Ang (1–7), angiotensin (1–7); SEM, standard error of mean.

the best nucleophile, while telmisartan is the best electrophile, see Table 2**.** Regarding the binding energy of the drugs with the three amino acids, the binding energies are larger than in the complex of the RBD of SARS-CoV-2 with ACE2; however, the ordering remains almost the same, which is characteristic of the binding ability of the drugs, i.e., telmisartan > ACC519T(2) > candesartan > ACC519T > losartan carboxylic acid > BV6 > losartan > nirmatrelvir (Table 2**).** From these results, we can see that telmisartan and ACC519T(2) favor the stronger binding with the active center of ACE2. They have the most negatively charged N atoms in tetrazole that accept H^+, showing that the hydrogen cation of the guanidinium group of Arg273 can more easily be accepted.

The study showed that proton transfer in peptide dimers is energetically unfavorable. The corresponding transition states are almost degenerate in energy with the products, and the potential energy surfaces of hydrogen transfer are shallow. The shorter hydrogen bonds in the dimers stabilize the transition states. Consequently, even if the proton is transferred, it returns to its original amino acid. The BE of the peptide dimers are −7.59 kcal/mol (Tyr-H…His-H) and −9.12 kcal/mol (His-H…Phe), as seen in Table 4**.** In contrast, H^+ transfer in the peptide trimer is feasible. The proton is transferred from Tyr-H to His-H via the Tyr….H….His-H….Phe transition state, and then the second H^+ is transferred via the Tyr….H….His…H….Phe transition state. The energetic demands are minimal, namely 3.6 kcal/mol and an additional 2.9 kcal/mol. The BE of the Tyr-H…His-H…Phe complex and the Tyr…H-His…Phe-H complex relative to the corresponding involved monomers are −16.15 and −29.29 kcal/mol, respectively. Despite the Tyr…H-His…Phe-H complex being 5.1 kcal/mol higher in energy than the Tyr-H…His-H…Phe complex, its BE is 13.2 kcal/mol greater than that of the Tyr-H…His-H…Phe complex. The infrared spectra of the Tyr-H…His-H…Phe and Tyr…H-His…Phe-H complexes are shown in Fig. 7. Both are true minima, with no imaginary frequencies. The first normal mode frequency, a bend motion of the peptide trimer, is only 4 cm-1. Normal mode frequencies corresponding to the stretching of the covalent hydrogen bond, where the H^+ is transferred between amino acids, are provided in Table 4. The study finds that the H bond stretching of Tyr-H-His is higher in energy than the H bond stretching of His-H-Phe in both minima. Additionally, in the Tyr-H…His-H…Phe peptide trimer, the normal modes are higher in energy compared to Tyr…H-His…Phe-H, indicating a greater energy requirement for proton transfer in the first complex. However, even for the higher-energy normal mode of H covalent bond stretching at 3039 cm-1 (8.69 kcal/mol), the energy demand is covered by the BE of the Tyr…H-His…Phe-H. In summary, while proton transfer in dimers is not favorable, it is possible in the peptide trimer, despite the Tyr…H-His…Phe-H complex being 5.1 kcal/mol higher in energy than the Tyr-H…His-H…Phe complex. The BE of the Tyr-H…His-H…Phe complex is −16.1 kcal/mol, while after the H + transfer, the BE of the Tyr…H-His…Phe-H complex is −29.3 kcal/mol, indicating a favorable proton transfer.

RAS induced hypertension plays a crucial role in exacerbating the pathophysiological hallmarks of COVID-19. Hypertension is considered one of the most common comorbidities in COVID-19 patients with a reported prevalence of 30 % in hospital admitted patients [46]. As SARS-CoV-2 relies predominantly on ACE2 to enter host cells, inhibiting this interaction has been suggested as an attractive pharmacological target in the prevention of SARS-CoV-2 infection; however, as the enzymatic function of ACE2 plays a protective role against multiple disease states, including hypertension and inflammation, it is important to clarify if the sartan-ACE2 interactions determined by DFT is associated with an effect on enzyme function. Various studies have shown that Arg237 is critical for substrate binding, such that its replacement causes enzyme activity to be abolished [47]. Additionally, Arg273 is also identified to form a salt-bridge with the C-terminus of potent ACE2 inhibitor MLN-4760 to induce conformation changes to prevent substrate binding [48]. Thus, it was important to assess if the affinity of sartans to Arg273 in the active site of ACE2 as calculated by DFT would induce antagonistic activity. Considering the protective effects elicited by ACE2 in homeostatic physiology, inhibiting its enzymatic function may be undesirable, as this could contribute to an increase in deleterious AngII-mediated

cardiovascular and renal effects [49–52]. Importantly, we revealed that the majority of sartans, including telmisartan and ACC519T(2) (which contained the highest calculated affinity to the active site of ACE2) where not capable in inhibiting enzyme activity, suggesting that the affinity of these compounds to active site of ACE2 is not associated with modulation of enzymatic function (Table 5, Fig. 9). This agrees with a recent study showing that there is no relationship between the affinity of compounds to the active site of ACE2 and functional capabilities [17]. The lack of sartan antagonism may be due to an absence in H^+-bonding with residuals His345 and His505 which have been identified as critical amino acids in the active site of ACE2, involved in both hydrolysis of AngII into Ang(1–7) and inhibitor binding [36,53].

We also showed that the ability of two sartans, namely candesartan and BV6$(K^+)_2$, significantly amplified rhACE2 activity (Table 5 and Fig. 9), for which BV6$(K^+)_2$ was shown to have 2.7-fold higher potency (Fig. 10). Despite the therapeutic potential of ACE2 activators, only a number of identified agents currently exist [54,55]. Docking studies in the literature have revealed that there are three primary allosteric binding sites capable of enhancing ACE2 activity [56]. Allosteric site 1 is located in close proximity to the active site, and contains an overwhelmingly higher affinity than the other two sites to putative ACE2 activators [53,55–57], thus this location is suggested to be the primary target for therapeutic intervention. This site may also be of possible interest to explain the ability of candesartan and BV6$(K^+)_2$ to increase ACE2 activity. The use of molecular dynamic simulations may be required to elude this mechanism of sartan-ACE2 interaction. The amplification of ACE2 activity results in an increased degradation of AngII to Ang(1–7) and could provide another approach to modify RAS dysfunction in addition to the well-established role of the sartans to inhibit the AT1R. Therefore, candesartan and BV6$(K^+)_2$ may be a more appropriate therapeutic approaches to treat hypertension, kidney disease, and inflammation.

Interestingly, nirmatrelvir, the antiviral protease inhibitor in Pfizer's COVID-19 drug, appeared to marginally inhibit rhACE2 activity, as shown in Fig. 9 and Table 5. This was evidenced by a slight increase in AngII and a decrease in Ang(1–7) compared to the positive control. Although the differences in peptide concentration did not reach statistical significance, various toxicological studies have concluded that nirmatrelvir is generally well tolerated [58,59]. Paxlovid is not recommended for patients with impaired kidney function [60], and is known to have a blood pressure elevating effect [58,61], which may be in part be related to a potential inhibitory interaction with ACE2. Nonetheless, the greater ACE2 binding affinities of sartans over nirmatrelvir as well as their ability to potential increase ACE2 activity in tissue (i.e., candesartan and BV6$(K^+)_2$) may indicate them that a more suitable candidate in the management of COVID-19.

5. Conclusion

Through the use of DFT methodology, we calculated the binding affinities of eight drugs with three key amino acids from the active stie of ACE2, aiming to identify potent candidates to prevent SARS-CoV-2 infection. Additionally, an *in vitro* enzymatic assay evaluated the impact of these compounds on ACE2 functional enzymatic activity to provide target compounds for COVID-19 therapy. Our findings indicate that telmisartan and ACC519T(2) showed the most promising antiviral effects, demonstrated by their strong binding affinities to ACEs's active centre. The ranking of the drugs, from most to least effective, was determined as, telmisartan > ACC519T(2) > candesartan > ACC519T > losartan carboxylic acid > BV6 > losartan > nirmatrelvir. Various reactivity descriptors and proton transfer dynamics among amino acids of the active center, where these drugs bind was studied. Proton transfer in the peptide dimers was not favored but occurred in peptide timers. Furthermore, our analysis confirmed that candesartan and BV6$(K^+)_2$ could beneficially enhance ACE2 activity. In summary, the accumulated *in silico* and *in vitro* data support the multi-functional roles of sartans. These compounds not only inhibit the interaction between S protein and ACE2 but also offer protective effects by modulating the RAS, inhibiting AngII/AT1R signaling, and promoting Ang(1–7)/MasR signaling.

CRediT authorship contribution statement

Vasso Apostolopoulos: Writing – review & editing, Writing – original draft, Conceptualization. **Nikitas Georgiou:** Writing – review & editing, Writing – original draft, Methodology. **Demeter Tzeli:** Writing – review & editing, Writing – original draft, Methodology, Conceptualization. **Thomas Mavromoustakos:** Writing – review & editing, Writing – original draft. **Graham J. Moore:** Writing – review & editing, Writing – original draft, Methodology, Conceptualization. **Konstantinos Kelaidonis:** Writing – review & editing, Methodology. **Minos-Timotheos Matsoukas:** Writing – review & editing. **Sotirios Tsiodras:** Writing – review & editing. **Jordan Swiderski:** Writing – review & editing, Writing – original draft, Methodology. **Laura Kate Gadanec:** Writing – review & editing, Writing – original draft, Methodology. **Anthony Zulli:** Writing – review & editing, Writing – original draft, Methodology. **Christos T. Chasapis:** Writing – review & editing, Writing – original draft, Methodology, Conceptualization. **John M. Matsoukas:** Writing – review & editing, Writing – original draft, Methodology, Conceptualization.

Declaration of competing interest

The authors declare that they have no known competing financial interests or personal relationships that could have appeared to influence the work reported in this paper.

Data availability

The computational and *in vitro* datasets, including DFT calculations and HPLC studies, used and/or analyzed in this study are publicly available at https://zenodo.org/ (https://doi.org/10.5281/zenodo.10660115). Software used in the manuscript for analysis of data are third party software packages that can be found at https://www.graphpad.com/scientific-software/prism/www.graphpad.com/scientific-software/prism/ (HPLC statistical analysis) and https://gaussian.com/gaussian16/ (DFT calculations).

Acknowledgments

J.M.M. and K.K. would like to express their gratitude to start-up company New Drug /NeoFar located at Patras Science Park, Greece, for providing the personnel and the infrastructure to develop bisartans the new generation of antivirals. They also thank Elevate Greece and the Region of Western Greece (Research and Technology) for funding (NeoFar financial support through MIS 5092131-action 110051339 grant) and their invaluable support throughout all the necessary steps in the implementation of the current research. C.T.C. would like to thank the National Research Foundation (NHRF) for supporting the research work by providing a Research Seed Grant. V.A. was supported through the Vice-Chancellors Distinguished Fellows scheme, Victoria University. L.K.G and J.S. were supported by the Victoria University Postgraduate scholarship. V.A. was also supported by a Planetary Health Grant PH098 from Victoria University. V.A. would like to thank the Greek Orthodox Archdiocese of Australia Funds, whose generous support made possible the research of this paper. The team would like to acknowledge the pan-antiviral ELPanvir Consortium for their support and ongoing discussions.

Funding information

Not applicable.

Appendix A. Supplementary data

Supplementary data to this article can be found online at https://doi.org/10.1016/j.bioorg.2024.107602.

References

[1] A. Benigni, P. Cassis, G. Remuzzi, Angiotensin II revisited: new roles in inflammation, immunology and aging, EMBO Mol. Med. 2 (7) (2010) 247–257.
[2] C.H. Wu, S. Mohammadmoradi, J.Z. Chen, H. Sawada, A. Daugherty, H.S. Lu, Renin-angiotensin system and cardiovascular functions, Arterioscler. Thromb. Vasc. Biol. 38 (7) (2018) e108–e116.
[3] R.A.S. Santos, W.O. Sampaio, A.C. Alzamora, D. Motta-Santos, N. Alenina, M. Bader, M.J. Campagnole-Santos, The ACE2/angiotensin-(1–7)/MAS axis of the renin-angiotensin system: focus on angiotensin-(1–7), Physiol. Rev. 98 (1) (2018) 505–553.
[4] H.T. Cohen, A.P. Bress, A.M. South, Relationship between ACE2 and other components of the renin-angiotensin system, Curr. Hypertens. Rep. 22 (44) (2020).
[5] T.R. Rodrigues Prestes, N.P. Rocha, A.S. Miranda, A.L. Teixeira, E.S.A.C. Simoes, The anti-inflammatory potential of ACE2/angiotensin-(1–7)/Mas receptor axis: evidence from basic and clinical research, Curr. Drug Targets 18 (11) (2017) 1301–1313.
[6] A.C. Simoes e Silva, K.D. Silveira, A.J. Ferreira, M.M. Teixeira, ACE2, angiotensin-(1–7) and Mas receptor axis in inflammation and fibrosis, Br. J. Pharmacol. 169 (3) (2013) 477–492.
[7] J.C. Zhong, D.Y. Huang, Y.M. Yang, Y.F. Li, G.F. Liu, X.H. Song, K. Du, Upregulation of angiotensin-converting enzyme 2 by all-trans retinoic acid in spontaneously hypertensive rats, Hypertension 44 (6) (2004) 907–912.
[8] M.A. Crackower, R. Sarao, G.Y. Oudit, C. Yagil, I. Kozieradzki, S.E. Scanga, A. J. Oliveira-dos-Santos, J. da Costa, L. Zhang, Y. Pei, J. Scholey, C.M. Ferrario, A. S. Manoukian, M.C. Chappell, P.H. Backx, Y. Yagil, J.M. Penninger, Angiotensin-converting enzyme 2 is an essential regulator of heart function, Nature 417 (6891) (2002) 822–828.
[9] S.B. Gurley, A. Allred, T.H. Le, R. Griffiths, L. Mao, N. Philip, T.A. Haystead, M. Donoghue, R.E. Breitbart, S.L. Acton, H.A. Rockman, T.M. Coffman, Altered blood pressure responses and normal cardiac phenotype in ACE2-null mice, J. Clin. Invest. 116 (8) (2006) 2218–2225.
[10] Z.A. Abassi, K. Skorecki, S.N. Heyman, S. Kinaneh, Z. Armaly, Covid-19 infection and mortality: a physiologist's perspective enlightening clinical features and plausible interventional strategies, Am. J. Physiol. Lung Cell. Mol. Physiol. 318 (5) (2020) L1020–L1022.
[11] J. Guo, Z. Huang, L. Lin, J. Lv, Coronavirus disease 2019 (COVID-19) and cardiovascular disease: a viewpoint on the potential influence of angiotensin-converting enzyme inhibitors/angiotensin receptor blockers on onset and severity of severe acute respiratory syndrome coronavirus 2 infection, J. Am. Heart Assoc. 9 (7) (2020) e016219.
[12] J. Yang, S.J.L. Petitjean, M. Koehler, Q. Zhang, A.C. Dumitru, W. Chen, S. Derclaye, S.P. Vincent, P. Soumillion, D. Alsteens, Molecular interaction and inhibition of SARS-CoV-2 binding to the ACE2 receptor, Nat. Commun. 11 (1) (2020) 4541.
[13] E.F. Healy, M. Lilic, A model for COVID-19-induced dysregulation of ACE2 shedding by ADAM17, Biochem. Biophys. Res. Commun. 573 (2021) 158–163.
[14] K. Kuba, Y. Imai, T. Ohto-Nakanishi, J.M. Penninger, Trilogy of ACE2: a peptidase in the renin-angiotensin system, a SARS receptor, and a partner for amino acid transporters, Pharmacol. Ther. 128 (1) (2010) 119–128.
[15] J. Swiderski, L.K. Gadanec, V. Apostolopoulos, G.J. Moore, K. Kelaidonis, J. M. Matsoukas, A. Zulli, Role of angiotensin II in cardiovascular diseases: introducing bisartans as a novel therapy for coronavirus 2019, Biomolecules 13 (5) (2023).
[16] A.E. Schutte, T.H. Jafar, N.R. Poulter, A. Damasceno, N.A. Khan, P.M. Nilsson, J. Alsaid, D. Neupane, K. Kario, H. Beheiry, Addressing global disparities in blood pressure control: perspectives of the International Society of Hypertension, Cardiovasc. Res. 119 (2) (2023) 381–409.
[17] B. Fiorillo, S. Marchiano, F. Moraca, V. Sepe, A. Carino, P. Rapacciuolo, M. Biagioli, V. Limongelli, A. Zampella, B. Catalanotti, S. Fiorucci, Discovery of bile acid derivatives as potent ACE2 activators by virtual screening and essential dynamics, J. Chem. Inf. Model. 62 (1) (2022) 196–209.
[18] X. Liu, R. Raghuvanshi, F.D. Ceylan, B.W. Bolling, Quercetin and Its metabolites inhibit recombinant human angiotensin-converting enzyme 2 (ACE2) activity, J. Agric. Food Chem. 68 (47) (2020) 13982–13989.
[19] S. Laurent, Antihypertensive drugs, Pharmacol. Res. 124 (2017) 116–125.
[20] T. Mavromoustakos, A. Kolocouris, M. Zervou, P. Roumelioti, J. Matsoukas, R. Weisemann, An effort to understand the molecular basis of hypertension through the study of conformational analysis of losartan and sarmesin using a combination of nuclear magnetic resonance spectroscopy and theoretical calculations, J. Med. Chem. 42 (10) (1999) 1714–1722.
[21] F. Zhou, T. Yu, R. Du, G. Fan, Y. Liu, Z. Liu, J. Xiang, Y. Wang, B. Song, X. Gu, Clinical course and risk factors for mortality of adult inpatients with COVID-19 in Wuhan, China: a retrospective cohort study, Lancet 395 (10229) (2020) 1054–1062.
[22] G. Yang, Z. Tan, L. Zhou, M. Yang, L. Peng, J. Liu, J. Cai, R. Yang, J. Han, Y. Huang, S. He, Effects of angiotensin II receptor blockers and ACE (angiotensin-converting enzyme) inhibitors on virus infection, inflammatory status, and clinical outcomes in patients with COVID-19 and hypertension, Hypertension 76 (1) (2020) 51–58.
[23] P. Zhang, L. Zhu, J. Cai, F. Lei, J.-J. Qin, J. Xie, Y.-M. Liu, Y.-C. Zhao, X. Huang, L. Lin, M. Xia, M.-M. Chen, X. Cheng, X. Zhang, D. Guo, Y. Peng, Y.-X. Ji, J. Chen, Z.-G. She, Y. Wang, Q. Xu, R. Tan, H. Wang, J. Lin, P. Luo, S. Fu, H. Cai, P. Ye, B. Xiao, W. Mao, L. Liu, Y. Yan, M. Liu, M. Chen, X.-J. Zhang, X. Wang, R.M. Touyz, J. Xia, B.-H. Zhang, X. Huang, Y. Yuan, R. Loomba, P.P. Liu, H. Li, Association of inpatient use of angiotensin-converting enzyme inhibitors and angiotensin II receptor blockers with mortality among patients with hypertension hospitalized with COVID-19, Circ. Res. 126 (12) (2020) 1671–1681.
[24] G.J. Moore, H. Ridgway, K. Kelaidonis, C.T. Chasapis, I. Ligielli, T. Mavromoustakos, J. Bojarska, J.M. Matsoukas, Actions of novel angiotensin receptor blocking drugs, bisartans, relevant for COVID-19 therapy: biased agonism at angiotensin receptors and the beneficial effects of neprilysin in the renin angiotensin system, Molecules 27 (15) (2022).
[25] H. Ridgway, G.J. Moore, T. Mavromoustakos, S. Tsiodras, I. Ligielli, K. Kelaidonis, C.T. Chasapis, L.K. Gadanec, A. Zulli, V. Apostolopoulos, R. Petty, I. Karakasiliotis, V.G. Gorgoulis, J.M. Matsoukas, Discovery of a new generation of angiotensin receptor blocking drugs: receptor mechanisms and in silico binding to enzymes relevant to SARS-CoV-2, Comput. Struct. Biotechnol. J. 20 (2022) 2091–2111.
[26] H. Ridgway, G.J. Moore, L.K. Gadanec, A. Zulli, V. Apostolopoulos, W. Hoffmann, K. Węgrzyn, N. Vassilaki, G. Mpekoulis, M. Zouridakis, Novel benzimidazole angiotensin receptor blockers with anti-SARS-CoV-2 activity equipotent to that of nirmatrelvir: computational and enzymatic studies, Expert Opin. Therap. Targets (just-accepted) (2024).
[27] T. van Mourik, M. Buhl, M.P. Gaigeot, Density functional theory across chemistry, physics and biology, Philos. Trans. A Math. Phys. Eng. Sci. 372 (2011) (2014) 20120488.
[28] G.J. Moore, J.M. Pires, K. Kelaidonis, L.K. Gadanec, A. Zulli, V. Apostolopoulos, J. M. Matsoukas, Receptor interactions of angiotensin II and angiotensin receptor blockers-relevance to COVID-19, Biomolecules 11 (7) (2021).
[29] M. Frisch, G. Trucks, H. Schlegel, G. Scuseria, M. Robb, J. Cheeseman, J. Montgomery Jr, T. Vreven, K. Kudin, J. Burant, Gaussian, Inc., Wallingford, CT, 2004; C. Lee, W. Yang, RG Parr, Phys. Rev. B 37 (1988) 785.
[30] A.D. Becke, Density-functional thermochemistry. I. The effect of the exchange-only gradient correction, J. Chem. Phys. 96 (3) (1992) 2155–2160.
[31] J. Tirado-Rives, W.L. Jorgensen, Performance of B3LYP density functional methods for a large set of organic molecules, J. Chem. Theory Comput. 4 (2) (2008) 297–306.
[32] F. De Proft, P. Geerlings, Conceptual and computational DFT in the study of aromaticity, Chem. Rev. 101 (5) (2001) 1451–1464.
[33] S. Saha, R.K. Roy, P.W. Ayers, Are the Hirshfeld and Mulliken population analysis schemes consistent with chemical intuition? Int. J. Quantum Chem. 109 (9) (2009) 1790–1806.
[34] J. Tomasi, B. Mennucci, R. Cammi, Quantum mechanical continuum solvation models, Chem. Rev. 105 (8) (2005) 2999–3094.
[35] G. RA, 1, mj frisch, gw trucks, hb schlegel, ge scuseria, ma robb, jr cheeseman, g. Scalmani, v. Barone, b. Mennucci, ga petersson et al., gaussian, Inc, Wallingford CT 121 (2009) 150–166.
[36] J.L. Guy, R.M. Jackson, K.R. Acharya, E.D. Sturrock, N.M. Hooper, A.J. Turner, Angiotensin-converting enzyme-2 (ACE2): comparative modeling of the active site, specificity requirements, and chloride dependence, Biochemistry 42 (45) (2003) 13185–13192.
[37] G.I. Rice, D.A. Thomas, P.J. Grant, A.J. Turner, N.M. Hooper, Evaluation of angiotensin-converting enzyme (ACE), its homologue ACE2 and neprilysin in angiotensin peptide metabolism, Biochem. J. 383 (Pt 1) (2004) 45–51.
[38] Y. Polak, R.C. Speth, Metabolism of angiotensin peptides by angiotensin converting enzyme 2 (ACE2) and analysis of the effect of excess zinc on ACE2 enzymatic activity, Peptides 137 (2021) 170477.
[39] H. Ridgway, G.J. Moore, T. Mavromoustakos, S. Tsiodras, I. Ligielli, K. Kelaidonis, C.T. Chasapis, L.K. Gadanec, A. Zulli, V. Apostolopoulos, Discovery of a new generation of angiotensin receptor blocking drugs: Receptor mechanisms and in silico binding to enzymes relevant to SARS-CoV-2, Comput. Struct. Biotechnol. J. 20 (2022) 2091–2111.
[40] G.J. Moore, H. Ridgway, K. Kelaidonis, C.T. Chasapis, I. Ligielli, T. Mavromoustakos, J. Bojarska, J.M. Matsoukas, Actions of novel angiotensin receptor blocking drugs, bisartans, relevant for COVID-19 therapy: biased agonism at angiotensin receptors and the beneficial effects of neprilysin in the renin angiotensin system, Molecules 27 (15) (2022) 4854.
[41] K. Kelaidonis, I. Ligielli, S. Letsios, V.P. Vidali, T. Mavromoustakos, N. Vassilaki, G. J. Moore, W. Hoffmann, K. Węgrzyn, H. Ridgway, Computational and enzymatic studies of sartans in SARS-CoV-2 spike RBD-ACE2 Binding: the role of tetrazole and perspectives as antihypertensive and COVID-19 therapeutics, Int. J. Mol. Sci. 24 (9) (2023) 8454.
[42] J. Swiderski, L.K. Gadanec, V. Apostolopoulos, G.J. Moore, K. Kelaidonis, J. M. Matsoukas, A. Zulli, Role of angiotensin II in cardiovascular diseases: introducing bisartans as a novel therapy for coronavirus 2019, Biomolecules 13 (5) (2023) 787.
[43] H. Ridgway, C.T. Chasapis, K. Kelaidonis, I. Ligielli, G.J. Moore, L.K. Gadanec, A. Zulli, V. Apostolopoulos, T. Mavromoustakos, J.M. Matsoukas, Understanding the driving forces that trigger mutations in SARS-CoV-2: mutational energetics and the role of arginine blockers in COVID-19 therapy, Viruses 14 (5) (2022) 1029.
[44] H. Ridgway, C. Ntallis, C.T. Chasapis, K. Kelaidonis, M.-T. Matsoukas, P. Plotas, V. Apostolopoulos, G. Moore, S. Tsiodras, D. Paraskevis, Molecular epidemiology of SARS-CoV-2: the dominant role of arginine in mutations and infectivity, Viruses 15 (2) (2023) 309.
[45] J.M. Matsoukas, D. Panagiotopoulos, M. Keramida, T. Mavromoustakos, R. Yamdagni, Q. Wu, G.J. Moore, M. Saifeddine, M.D. Hollenberg, Synthesis and

contractile activities of cyclic thrombin receptor-derived peptide analogues with a Phe-Leu-Leu-Arg motif: importance of the Phe/Arg relative conformation and the primary amino group for activity, J. Med. Chem. 39 (18) (1996) 3585–3591.
[46] F. Zhou, T. Yu, R. Du, G. Fan, Y. Liu, Z. Liu, J. Xiang, Y. Wang, B. Song, X. Gu, L. Guan, Y. Wei, H. Li, X. Wu, J. Xu, S. Tu, Y. Zhang, H. Chen, B. Cao, Clinical course and risk factors for mortality of adult inpatients with COVID-19 in Wuhan, China: a retrospective cohort study, Lancet 395 (10229) (2020) 1054–1062.
[47] J.L. Guy, R.M. Jackson, H.A. Jensen, N.M. Hooper, A.J. Turner, Identification of critical active-site residues in angiotensin-converting enzyme-2 (ACE2) by site-directed mutagenesis, FEBS J. 272 (14) (2005) 3512–3520.
[48] N.A. Dales, A.E. Gould, J.A. Brown, E.F. Calderwood, B. Guan, C.A. Minor, J. M. Gavin, P. Hales, V.K. Kaushik, M. Stewart, P.J. Tummino, C.S. Vickers, T. D. Ocain, M.A. Patane, Substrate-based design of the first class of angiotensin-converting enzyme-related carboxypeptidase (ACE2) inhibitors, J. Am. Chem. Soc. 124 (40) (2002) 11852–11853.
[49] Y. Fang, F. Gao, Z. Liu, Angiotensin-converting enzyme 2 attenuates inflammatory response and oxidative stress in hyperoxic lung injury by regulating NF-kappaB and Nrf2 pathways, QJM 112 (12) (2019) 914–924.
[50] K. Kuba, Y. Imai, S. Rao, H. Gao, F. Guo, B. Guan, Y. Huan, P. Yang, Y. Zhang, W. Deng, L. Bao, B. Zhang, G. Liu, Z. Wang, M. Chappell, Y. Liu, D. Zheng, A. Leibbrandt, T. Wada, A.S. Slutsky, D. Liu, C. Qin, C. Jiang, J.M. Penninger, A crucial role of angiotensin converting enzyme 2 (ACE2) in SARS coronavirus-induced lung injury, Nat. Med. 11 (8) (2005) 875–879.
[51] Y. Qi, J. Zhang, C.T. Cole-Jeffrey, V. Shenoy, A. Espejo, M. Hanna, C. Song, C. J. Pepine, M.J. Katovich, M.K. Raizada, Diminazene aceturate enhances angiotensin-converting enzyme 2 activity and attenuates ischemia-induced cardiac pathophysiology, Hypertension 62 (4) (2013) 746–752.
[52] H.F. Hasan, E.M. Elgazzar, D.M. Mostafa, Diminazene aceturate extenuate the renal deleterious consequences of angiotensin-II induced by gamma-irradiation through boosting ACE2 signaling cascade, Life Sci. 253 (2020) 117749.
[53] K. Dutta, Allosteric site of ACE-2 as a drug target for COVID-19, ACS Pharmacol. Transl. Sci. 5 (3) (2022) 179–182.
[54] R. Rodriguez-Puertas, ACE2 activators for the treatment of COVID 19 patients, J. Med. Virol. 92 (10) (2020) 1701–1702.
[55] L.V. Kulemina, D.A. Ostrov, Prediction of off-target effects on angiotensin-converting enzyme 2, J. Biomol. Screen. 16 (8) (2011) 878–885.
[56] J.A. Hernandez Prada, A.J. Ferreira, M.J. Katovich, V. Shenoy, Y. Qi, R.A. Santos, R.K. Castellano, A.J. Lampkins, V. Gubala, D.A. Ostrov, M.K. Raizada, Structure-based identification of small-molecule angiotensin-converting enzyme 2 activators as novel antihypertensive agents, Hypertension 51 (5) (2008) 1312–1317.
[57] B.K. Maiti, Potential role of peptide-based antiviral therapy against SARS-CoV-2 infection, ACS Pharmacol. Transl. Sci. 3 (4) (2020) 783–785.
[58] W. Chen, B. Liang, X. Wu, L. Li, C. Wang, D. Xing, Advances and challenges in using nirmatrelvir and its derivatives against SARS-CoV-2 infection, J. Pharm. Anal. 13 (3) (2023) 255–261.
[59] D.R. Owen, C.M.N. Allerton, A.S. Anderson, L. Aschenbrenner, M. Avery, S. Berritt, B. Boras, R.D. Cardin, A. Carlo, K.J. Coffman, A. Dantonio, L. Di, H. Eng, R. Ferre, K.S. Gajiwala, S.A. Gibson, S.E. Greasley, B.L. Hurst, E.P. Kadar, A.S. Kalgutkar, J. C. Lee, J. Lee, W. Liu, S.W. Mason, S. Noell, J.J. Novak, R.S. Obach, K. Ogilvie, N. C. Patel, M. Pettersson, D.K. Rai, M.R. Reese, M.F. Sammons, J.G. Sathish, R.S. P. Singh, C.M. Steppan, A.E. Stewart, J.B. Tuttle, L. Updyke, P.R. Verhoest, L. Wei, Q. Yang, Y. Zhu, An oral SARS-CoV-2 M(pro) inhibitor clinical candidate for the treatment of COVID-19, Science 374 (6575) (2021) 1586–1593.
[60] S.S. Toussi, J.M. Neutel, J. Navarro, R.A. Preston, H. Shi, O. Kavetska, R. R. LaBadie, M. Binks, P.L.S. Chan, N. Demers, B. Corrigan, B. Damle, Pharmacokinetics of oral nirmatrelvir/ritonavir, a protease inhibitor for treatment of COVID-19, in subjects with renal impairment, Clin. Pharmacol. Ther. 112 (4) (2022) 892–900.
[61] E.G. McDonald, T.C. Lee, Nirmatrelvir-ritonavir for COVID-19, CMAJ 194 (6) (2022) E218.